Published article:

Wareing, CJ, Zijlstra, AA, Speck, AK, O'Brien, TJ, Ueta, T, Elitzur, M, Gehrz, RD, Herwig, F, Izumiura, H, Matsuura, M, Meixner, M, Stencel, RE and Szczerba, R (2006) *Detached shells as tracers of AGB-ISM bow shocks.* Monthly Notices Letters of the Royal Astronomical Society, 372 (1). L63 - L67. ISSN 1745-3933
http://dx.doi.org/10.1111/j.1745-3933.2006.00227.x

Mon. Not. R. Astron. Soc. **372**, L63–L67 (2006) doi:10.1111/j.1745-3933.2006.00227.x

Detached shells as tracers of asymptotic giant branch–interstellar medium bow shocks

C. J. Wareing,[1⋆] Albert A. Zijlstra,[1] Angela K. Speck,[2] T. J. O'Brien,[1] Toshiya Ueta,[3] M. Elitzur,[4] R. D. Gehrz,[5] F. Herwig,[6] H. Izumiura,[7] M. Matsuura,[8] M. Meixner,[9] R. E. Stencel[10] and R. Szczerba[11]

[1]*Jodrell Bank Centre for Astrophysics, University of Manchester, Oxford Road, Manchester, M13 9PL*
[2]*Department of Physics and Astronomy, 223 Physics Building, University of Missouri, Columbia, MO 65211, USA*
[3]*NASA Ames Research Center/USRA SOFIA Office, Mail Stop 211-3, Moffett Field, CA 94035, USA*
[4]*Physics & Astronomy Department, University of Kentucky, Lexington, KY 40506, USA*
[5]*Department of Astronomy, School of Physics and Astronomy, 116 Church Street, S.E., University of Minnesota, Minneapolis, MN 55455, USA*
[6]*Theoretical Astrophysics Group, LANL, Los Alamos, NM 87545, USA*
[7]*Okayama Astrophysical Observatory, National Astronomical Observatory of Japan, Kamogata, Asakuchi, Okayama 719-0232, Japan*
[8]*Division of Optical and IR Astronomy, National Astronomical Observatory of Japan, Osawa 2-21-1, Mitaka, Tokyo 181-8588, Japan*
[9]*STScI, 3700 San Martin Dr., Baltimore, MD 21218, USA*
[10]*Department of Physics and Astronomy, University of Denver, Denver, CO 80208, USA*
[11]*N. Copernicus Astronomical Centre, Rabianska 8, 87-100, Torun, Poland*

Accepted 2006 July 31. Received 2006 July 21; in original form 206 June 30

ABSTRACT

New *Spitzer* imaging observations have revealed the structure around the Mira variable star R Hya to be a one-sided parabolic arc 100 arcsec to the west, stretching from north to south. We successfully model R Hya and its surroundings in terms of an interaction of the stellar wind from an asymptotic giant branch (AGB) star with the interstellar medium (ISM) the star moves through. Our three-dimensional hydrodynamic simulation reproduces the structure as a bow shock into the oncoming ISM. We propose this as another explanation of detached shells around such stars, which should be considered alongside current theories of internal origin. The simulation predicts the existence of a tail of ram-pressure-stripped AGB material stretching downstream. Indications for such a tail behind R Hya are seen in *IRAS* maps.

Key words: stars: AGB and post-AGB – stars: individual: R Hya – stars: mass-loss – ISM: structure.

1 INTRODUCTION

Large detached shells have been observed around several asymptotic giant branch (AGB) stars. They have been seen in *IRAS* images of dust emission (Waters et al. 1994; Izumiura et al. 1997), CO line emission (Olofsson et al. 1996; Schöier, Lindqvist & Olofsson 2005) and, in a few cases, [Na I] and [K I] emission as well as in the optical continuum (González Delgado et al. 2001, 2003). Olofsson et al. (1990) suggested that such shells are the result of mass-loss variations and in particular a thermal pulse or He-flash. During a He-flash, an intense short-lived mass ejection is driven by the star reaching a critical luminosity. Thermal pulses are separated by phases of quiescent hydrogen burning lasting 10^4–10^5 yr. The stellar evolution tracks calculated by Vassiliadis & Wood (1993) confirmed that mass-loss fluctuations during the thermal pulse cycle can lead to detached circumstellar shells. Hydrodynamic simulations by Steffen & Schönberner (2000) showed that a brief period of high mass loss can translate into a geometrically thin shell expanding around the star. This has become the standard explanation of detached dust shells around stars and observations have been interpreted as such (Zijlstra et al. 1992; Speck, Meixner & Knapp 2000).

A separate explanation for large detached shells is the interaction of the AGB wind with the interstellar medium (ISM) (Young, Phillips & Knapp 1993). Zijlstra & Weinberger (2002) used this for a giant (∼4 pc at D ∼700 pc) detached shell surrounding an M3 III AGB star. They proposed that its AGB wind has been stopped by the surrounding ISM and the swept-up 'wall' is now expanding at the local sound speed. Simulations by Villaver, Garcia-Segura & Manchado (2003) and Wareing et al. (2006) confirmed the viability of this mechanism. It is likely that both mechanisms occur, but whether the external mechanism of an ISM wall or the internal mechanism of long-term mass-loss variations is the dominant cause of detached shells is not known. Schöier et al. (2005) found that the derived masses of the shells increase and the expansion velocities decrease with increasing radial distance from the star. They suggest

⋆E-mail: cwareing@jb.man.ac.uk

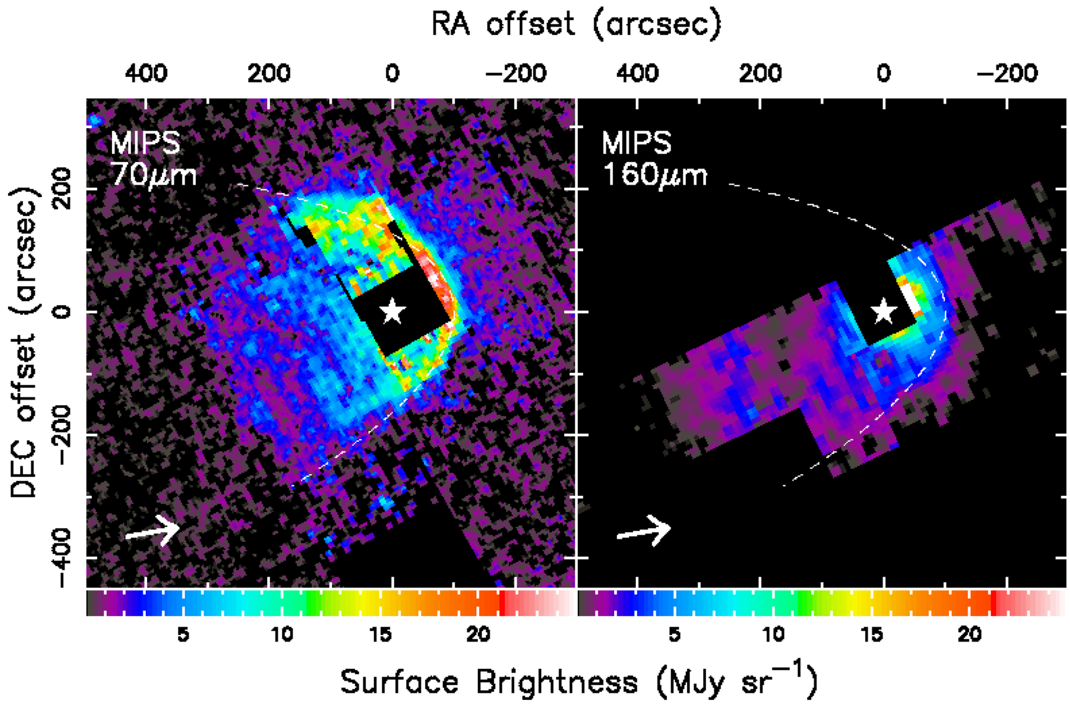

Figure 1. The background-subtracted, mosaicked MIPS colour maps of R Hya at 70 μm (left) and 160 μm (right) (Ueta et al. 2006). The images are zeroed at the position of the star (indicated by the 'star'), with north up and east to the left. The proper motion is indicated by the arrow in the bottom left. The parabolic arc is marked for clarity by the dashed line. Colour-scaling of surface brightness (in MJy sr^{-1}) is provided by the colour bar.

that the shell is sweeping up surrounding material from an earlier mass-loss phase. However, ISM sweep-up could yield similar effects.

A difference between the two mechanisms is that the internal one will normally give a spherical shell, while external mechanism will give a shape which depends on the motion of the star through the ISM. This is a testable prediction, if the proper motion of the star is known. Here we show that the detached shell around the Mira variable R Hya is due to an ISM bow shock.

2 OBSERVATIONS

R Hya is one of the brightest Mira variables on the sky. Hashimoto et al. (1998) found evidence in *IRAS* data for a detached shell 1–2 arcmin from the star. The star itself coincides with an *IRAS* point source due to an inner dust shell. This inner shell is also detached from the star, with an inner radius of about 60 stellar radii. Since its discovery in AD 1662, the pulsation period has decreased from 495 to 385 d, attributed to non-linear pulsation or a recent thermal pulse (Zijlstra, Bedding & Mattei 2002). The inner detachment suggests a mass-loss interruption occurred around AD 1800. The outer shell has a dynamical age of around 8000 yr. This small time-difference causes problems if one assumes that both detached shells are due to thermal pulses (Zijlstra et al. 2002).

The reported proper motion from the *Hipparcos* catalogue is 60.73 mas yr^{-1} west and 11.01 mas yr^{-1} north (Perryman et al. 1997). The radial velocity is −10.4 km s^{-1} (Wilson 1953). The distance to R Hya is uncertain, as discussed in section 4 of Zijlstra et al. (2002). Eggen (1985) argues for a distance of 165 pc based on a proper motion companion, but the data this is based on appears to be unpublished. The *Hipparcos* non-detection favours a larger distance. We have adopted a distance of 165 pc. This distance puts R Hya just beyond the edge of the Local Bubble in this direction (Lallement et al. 2003). At our chosen distance, the proper motion is equivalent to a transverse velocity of 48.5 km s^{-1}, and a space velocity of 49.5 km s^{-1}. This is within 2σ of the average space velocity for AGB stars, 30 km s^{-1} (Feast & Whitelock 2000).

High angular resolution observations were taken with the *Spitzer* Space Telescope (Werner et al. 2004) as part of the MIRIAD project (Ueta et al. 2006). The Multiband Imaging Photometer aboard *Spitzer* (MIPS; Rieke et al. 2004) image is shown in Fig. 1. The central unobserved region in the images avoids the central star which would saturate the detectors. For details of the data reduction process, please consult Ueta et al. (2006).

These images show that the material around the central star is not a circular shell as suggested by the *IRAS* observations (Hashimoto et al. 1998), but instead consists of a parabolic arc to the west of the star and regions of emission to the east. The arc appears brightest in the direction of the proper motion, fading as it stretches away north and south. At its brightest point, the arc is 100 arcsec from the central star. The arc is 300 arcsec wide across the star. There appears to be no emission further west of the arc, suggesting there is no material related to R Hya west of the arc. It is not clear from these images that the arc is detached from the star as the region between the arc and star is in the central unobserved region. To the east of the star, several low-brightness regions of emission are present up to 300 arcsec from the star. The location and brightness of these regions would suggest they are associated with the star. Our simulations closely reproduce the morphology of the arc and the eastern emission.

3 SIMULATIONS

Our simulations have been performed using a parallelized computational fluid dynamics program designed to solve the standard Euler equations of hydrodynamics using a second-order Godunov scheme due to Falle (1991). It is in three dimensions using Cartesian coordinates and includes the effect of radiative cooling above 10^4 K via a parametric fit to the cooling curve of Raymond, Cox & Smith (1976). The time-step is defined by the Courant–Friedrichs–Lewy condition with a Courant number of 0.5. We also include a numerical viscosity to avoid on-axis issues in the simulations.

Using this numerical scheme, we have modelled the interaction of a stellar wind ejected from a star as it moves through the ISM. The simulation is performed in the frame of reference of the star and the motion through the ISM is like that of an oncoming wind – hence our 'two-wind' model. Further details of the model are explained in Wareing et al. (2006). We model a period of 5.5×10^4 yr on the AGB and have used a simulation grid of 200^3 cubic cells (cell size of 4×10^{-3} pc) producing a grid of 0.8 pc in each direction.

We set the AGB wind parameters of the model with a mass-loss rate of $3 \times 10^{-7}\,M_{\odot}\,yr^{-1}$ and a velocity of $10\,km\,s^{-1}$ (Zijlstra et al. 2002). The temperature of the wind is set at 10^4 K, which is the lowest value for which the cooling function is defined (Wareing 2005). The real temperature will be considerably less than this, and indeed the temperature of the undisturbed AGB wind in the simulation is of the order of a few tens of K. Our simulations do not model dust physics or radiation transport. The gas pressure in both winds is calculated assuming an ideal gas equation of state with an adiabatic index of 5/3 in both winds, effectively ignoring molecules.

The position of the bow shock 0.08 pc ahead of the star at our adopted distance can be understood in terms of a ram pressure balance. This balance predicts a local ISM density of $n_H = 0.6\,cm^{-3}$ which we take as the ISM density in our simulations. The ISM is modelled as a warm neutral medium with a temperature of 8×10^3 K. The stellar motion corresponds to a Mach number of 3.65 and the AGB wind has a Mach number of 0.74. At 165 pc, R Hya is located 101 pc above the Galactic plane. ISM density, and hence pressure, is constant at $n_H = 2\,cm^{-3}$ (Spitzer 1978) up to a scaleheight of 100 pc (Binney & Merrifield 1998). Above this, density drops off exponentially, giving an ISM density in the region of R Hya of $0.74\,H\,cm^{-3}$ in accidental agreement with our simulation. This is also consistent with the estimate of $0.4\,H\,cm^{-3}$ calculated by Ueta et al. (2006). Densities within the Local Bubble would be very much lower: the bow shock supports a location of R Hya beyond this region.

4 RESULTS

Fig. 2 shows density on the plane in which the star is located 40 000 yr into the AGB phase. This point in time is an arbitrary choice as the wind structure reached a stable state after 25 000 yr into the simulation. The image is at 9°.5 to the actual line of sight to R Hya.

The wind from the star has driven a shock into the ISM. In the case of a stationary star, this is a spherical shell of AGB wind material sweeping up shocked ISM material. In the moving case, the shock forms into a bow shock expanding ahead of the star. Eventually, the bow shock reaches a maximum distance ahead of the star (after 25 000 yr in our simulation) which can be understood in terms of a ram pressure balance. Material is being ram-pressure-stripped from the head of the bow shock into a tail stretching downstream. The 'bow shock and tail' structure is the same as we have seen in other simulations considering a range of space velocities and wind parameters. We note this as support for the formation of this general structure as a convergent result.

The width of the bow shock across the star is approximately 0.24 pc, agreeing with the observations. If the bow shock is a strong shock, the temperature of the shocked material at the head can be

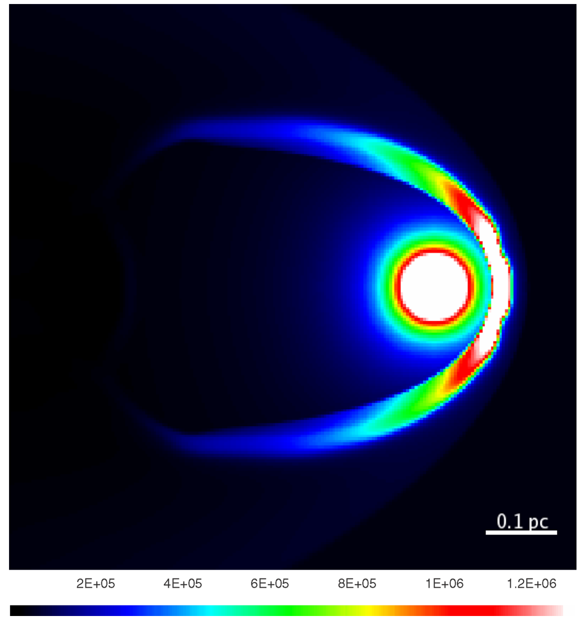

Figure 2. An image showing the gas density in the plane in which the star is located, parallel to the direction of motion, 40 000 yr into the simulation. The ISM is flowing in from the right. This image is at 9°.5 to the actual line-of-sight to R Hya. The colour bar is in units of $10^{-6}\,M_{\odot}\,pc^{-3}$ where 2.4×10^5 corresponds to $10\,H\,cm^{-3}$. The image is 0.8 pc on a side, which corresponds to the physical image scale in Fig. 1 at 165 pc.

predicted by $T \sim 3/16\,mv^2/k = 33\,000$ K, where m is taken as the average gas component mass of 1.0×10^{-27} kg, v is the speed of the central star relative to the ISM and k is the Boltzmann constant. The temperature in the simulation at the head of the bow shock is found to be in agreement with this prediction. The survival of dust above temperatures of approximately 1500 K is questionable, but at the low densities in the simulation the dust and gas are decoupled and evidently the dust temperature can be much lower.

5 DISCUSSION

5.1 The bow shock

The two-wind model can reproduce the appearance of the circumstellar structure around R Hya, with physical dimensions matching that of the bow shock. The head of the bow shock is in good agreement with the direction of motion. Small regions of emission downstream can be explained in terms of regions of higher density ISM encountered by the stellar wind. Such high-density regions in the ISM have been shown to survive ablation by stellar winds (Pittard et al. 2005).

In our simulation, we find a high temperature of 35 000 K at the head of the bow shock, with material cooling rapidly as it moves down the tail. The high temperatures are consistent with the observed Hα emission (Gaustad et al. 2001; Ueta et al. 2006). The high temperatures will affect the dust by collisional heating. However, it is impossible for us to say whether this heat from the local gas is more important than the stellar radiation or the interstellar radiation field (Speck et al. 2000) in controlling the dust temperature.

The *Spitzer* and *IRAS* images indicate that the bow-shock region is detected through dust emission; the fact that the emission is strongest at 60 μm indicates a dust temperature of the order of 60 K. However, other emission processes may play a role. Shocked regions can show [O I] 63- and 146-μm lines. The *IRAS* 100-μm detection (Hashimoto et al. 1998), in a band without strong lines, shows that dust contributes to the far-infrared emission.

5.2 Other cases: mass-loss variations versus ISM interaction

Cases of detached shells around AGB stars include U Ant (Izumiura et al. 1997), U Hya (Waters et al. 1994), Y CVn (Izumiura et al. 1996), R Hya (Hashimoto et al. 1998) and IRAS 02091+6333 (Zijlstra & Weinberger 2002) observed in the far-infrared, and detached molecular (CO) gas shells around TT Cyg, S Sct, R Scl, U Ant, U Cam, V644 Sco and DR Ser (Olofsson et al. 1996; Schöier et al. 2005). All are carbon stars, apart from R Hya and IRAS 02091+6333. It has been suggested that the thermal pulse scenario may only lead to mass-loss spikes for carbon stars (Schöier et al. 2005) but this is very much dependent on the assumed mass loss prescription which is not well known. *IRAS* colours indicate that detached shells do also exist around oxygen-rich stars (Zijlstra et al. 1992) and many more stars are likely to show large shells (Young et al. 1993).

An interesting comparison can be made between R Hya and U Hya. U Hya has a thin circular shell with a radius of 120 arcsec (Waters et al. 1994). It has a space velocity of 50 km s^{-1} and the parallax gives a distance of 162 pc (Perryman et al. 1997). The circular nature of the shell suggests an internal origin such as the mass-loss variations proposed by, for example, Zijlstra et al. (1992) and Schöier et al. (2005). The age of the shell in this particular case is 6000 yr. The ISM interaction may be radially further away from the star.

The star TT Cyg is surrounded by a circular detached shell at a radius of approximately 40 arcsec (Olofsson et al. 1996); the physical size of the shell is very similar to U Hya, in view of the larger distance of TT Cyg. The thin symmetrical appearance supports an internal origin. Interestingly, the space motion of TT Cyg (50 km s^{-1}) is almost all in the radial direction away from us and any bow shock formed by an interaction with the ISM would appear circular on the sky. But the fact that the slight offset of the star from the centre of the shell is at right angles to the direction of proper motion, favours an internal origin in mass-loss variations.

For other stars there is insufficient data to decide on the cause of the detached shells. It may be that the well-studied carbon stars with detached shells are mostly due to internal mechanisms, i.e. thermal pulses, while the fainter, less studied shells are dominated by ISM interactions. CO observations of shells around carbon stars reveal relatively high velocities (about 20 km s^{-1}) which favours thermal pulse origins (Olofsson et al. 1996; Schöier et al. 2005). Multiple detached shells do exist in the AGB phase of evolution, e.g. S Sct and U Ant (González Delgado et al. 2003) and also R Hya: thus, both mechanisms may occur simultaneously.

Young et al. (1993) in their analysis of 76 AGB stars resolved by *IRAS* found no evidence for distortions by interaction with the ISM. Because R Hya is included in their sample, this lack of evidence can be attributed to the poor spatial resolution and image quality of the *IRAS* instrument.

R Hya can be considered a typical case for the mass-loss rate and ISM density although its space velocity is perhaps high. Lower velocity objects will have a bow shock and with higher mass-loss rates this will be located further from the star. In a zero-velocity case, the bow shock transforms into a spherical swept-up shell of ISM material (Young et al. 1993; Speck et al. 2000; Zijlstra & Weinberger 2002). We predict that all AGB stars will show some degree of an AGB–ISM interaction, although bow shocks will be rarer. The interpretation of a detached shell in terms of a mass-loss variation must be considered with this ISM interaction in mind.

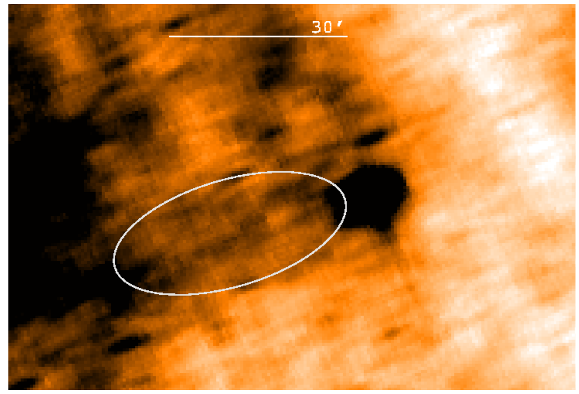

Figure 3. A figure showing an *IRAS* 60-μm observation of the area around R Hya. North is up and east to the left. Evidence for a tail of material is indicated by the ellipse.

5.3 Mass loss history

This model has shown that information usually gleaned from circumstellar dust shells around Mira variables can no longer be inferred in this situation. The bow shock has destroyed any mass-loss history older than about 10^4 yr in the case of R Hya. A higher mass-loss rate and/or lower ISM density could increase this time-scale, as found by Young et al. (1993) and Zijlstra & Weinberger (2002).

The simulations predict the occurrence of a tail, consisting of swept-back ISM and stellar wind gas. The mass-loss history can in principle still be traced down the length of the tail. *IRAS* maps provide some indication for a tenuous detection of material downstream of R Hya as shown in Fig. 3. This material stretches up to 30 arcmin away or 1.5 pc at a distance of 165 pc. At 49.5 km s^{-1} this implies a minimum tail age of 30 000 yr. Adding the 25 000 yr it takes to form the stable bow shock, to represent the travel time from the star to the bow shock and down the tails, we predict R Hya has been losing mass for at least 55 000 yr.

If we consider it has taken 25 000 yr to form the bow shock and after this the bow shock is in a steady state, an appreciable amount of mass is in the bow shock. The estimate from the simulation is 2.6×10^{-3} M$_{\odot}$ in the region of the bow shock, defined as a hemispherical upwind shell centred on the star with inner radius of 0.08 pc and a thickness of 0.1 pc. Our analytical estimate of the mass in the bow shock is consistent with this estimate, suggesting there is four times more stellar mass in the bow shock than ISM mass. At a dust temperature of 60 K and assuming a dust-to-gas ratio of 100, we predict a 100-μm flux of 15 Jy, in broad agreement with the fluxes observed by Ueta et al. (2006).

We use a constant stellar mass-loss rate and wind velocity. However, the dust shell models of various people (Zijlstra & Weinberger 2002; Schöier et al. 2005) indicate that these quantities are variable, particularly during the thermal pulses. Models indicate that in the course of thermal pulses the stellar radius changes temporarily by a factor of 2, and the mass-loss rate by an order of magnitude, causing a density and velocity spike moving radially away from the star that is considered as the origin of detached dust shells. Such events could severely disturb the pressure balance that dictates the well-defined location of the bow shock when one of these 'wind'-shells runs into the bow shock. There is likely to be a complex time-dependence of the wind-ISM interaction on the time-scales of the thermal pulses, as has been considered in two-dimensional simulations by Villaver et al. (2003).

ACKNOWLEDGMENTS

The numerical computations in this work were carried out using the COBRA supercomputer at Jodrell Bank Observatory. The *Spitzer* Space Telescope is operated by the JPL/Caltech under a contract with NASA. We acknowledge additional support for the following individuals: Speck – NASA ADP grant (NAG 5-12675), Ueta – NPP Research Fellowship Award, Elitzur – NSF Grant: AST–0507421, Gehrz – in part by NASA (Contract 1215746) issued by JPL/Caltech to Gehrz to the University of Minnesota, Herwig – LDRD program (20060357ER) at LANL, Izumiura – Grant-in-Aid (C) from JSPS (No.17540221), Matsuura – JSPS, Stencel – in part by NASA (Contract 1275979) issued by JPL/Caltech to the University of Denver, Szczerba – grant 2.P03D.017.25, Wareing – PPARC.

REFERENCES

Binney J., Merrifield M., 1998, Galactic Astronomy. Princeton University Press, Princeton, ch. 10
Eggen O. J., 1985, AJ, 90, 333
Falle S. A. E. G., 1991, MNRAS, 250, 581
Feast M. W., Whitelock P. A., 2000, MNRAS, 317, 460
Gaustad J. E., McCullough P. R., Rosing W., Van Buren D., 2001, PASP, 113, 1326
González Delgado D., Olofsson H., Schwarz H. E., Eriksson K., Gustafsson B., 2001, A&A, 372, 885
González Delgado D., Olofsson H., Schwarz H. E., Eriksson K., Gustafsson B., Gledhill T., 2003, A&A, 399, 1021
Hashimoto O., Izumiura H., Kester D. J. M., Bontekoe T. R., 1998, A&A, 329, 213
Izumiura H., Hashimoto O., Kawara K., Yamamura I., Waters L. B. F. M., 1996, A&A, 315, L221
Izumiura H., Waters L. B. F. M., de Jong T., Loup C., Bontekoe Tj. R., Kester D. J. M., 1997, A&A, 323, 449
Lallement R., Welsh B. Y., Vergely J. L., Crifo F., Sfeir D., 2003, A&A, 411, 447
Olofsson H., Carlstrom U., Eriksson K., Gustafsson B., Willson L. A., 1990, A&A, 230, L13
Olofsson H., Bergman P., Eriksson K., Gustafsson B., 1996, A&A, 311, 587
Perryman M. A. C. et al., 1997, A&A, 323, L49
Pittard J. M., Dyson J. E., Falle S. A. E. G., Hartquist T. W., 2005, MNRAS, 361, 1077
Raymond J. C., Cox D. P., Smith B. W., 1976, ApJ, 204, 290
Rieke G. H. et al., 2004, ApJS, 154, 25
Schöier F. L., Lindqvist M., Olofsson H., 2005, A&A, 436, 633
Speck A. K., Meixner M., Knapp G. R., 2000, ApJ, 545, L145
Spitzer L., Jr., 1978, Physical Processes in the Interstellar Medium. New York, Wiley, p. 234
Steffen M., Schönberner D., 2000, A&A, 357, 180
Ueta T. et al. 2006, ApJL, in press
Vassiliadis E., Wood P., 1993, ApJ, 413, 641
Villaver E., Garcia-Segura G., Manchado A., 2003, ApJ, 585, L49
Waters L. B. F. M., Loup C., Kester D. J. M., Bontekoe T. R., de Jong T., 1994, A&A, 281, L1
Wareing C. J., 2005, PhD thesis, Univ. Manchester
Wareing C. J., O'Brien T. J., Zijlstra A. A., Kwitter K. B., Irwin J., Wright N., Greimel R., Drew J., 2006, MNRAS, 366, 387
Werner M. W. et al., 2004, ApJS, 154, 1
Wilson R. E., 1953, General Catalogue of Stellar Radial Velocities. Carnegie Institute, Washington DC
Young K., Phillips T. G., Knapp G. R., 1993, ApJ, 409, 725
Zijlstra A. A., Weinberger R., 2002, ApJ, 572, 1006
Zijlstra A. A., Loup C., Waters L. B. F. M., de Jong T., 1992, A&A, 265, L5
Zijlstra A. A., Bedding T. R., Mattei J. A., 2002, MNRAS, 334, 498

This paper has been typeset from a TEX/LATEX file prepared by the author.